

内共振条件下直线运动梁的动力稳定性¹⁾

冯志华 胡海岩

(南京航空航天大学振动工程研究所, 南京 210016)

摘要 基于 Kane 方程, 建立起了包含有耦合的三次几何及惯性非线性项大范围直线运动梁动力学控制方程。利用多尺度法并结合笛卡尔坐标变换, 对所得方程进行一次近似展开, 着重对满足一、二阶模态间 3:1 内共振现象的两端饺支梁参激振动平凡解稳定性进行了详尽的分析, 得出了稳定性边界的解析表达式。采用中心流形定理对调制微分方程组进行降维处理, 分析了相应 Hopf 分岔类型并通过数值计算发现了稳定的极限环存在。

关键词 梁, 动力稳定性, 参激振动, 内共振, 多尺度法, 大范围直线运动

引言

承受一定惯性载荷的大范围直线运动弹性结构在军事、航空航天等工业中随处可见。然而, 对于此类环境中弹性结构动力学问题的研究, 即使是其最简单的结构形式之一——梁的动力行为的研究, 也鲜有报道。Kane 等较早地建立了非惯性场中悬臂梁的动力学方程, 但在方程的建立过程中引进了一些线性化的处理手段, 且所举例子仅局限于大范围的转动^[1]。Nayfeh 及 Mook 采用多尺度法一次近似展开, 对轴向激励悬臂梁参激振动稳定性问题进行了系统的研究与归纳^[2]。Hyun 等采用多尺度法二次近似展开, 对文献[2]所述对象的稳定性问题作了更细致的研究^[3]。文献[2]与[3]只考虑了线性化的方程组, 故对模态间因存在内共振现象而可能导致复杂的参激振动稳定性问题未给予关注。最近, 冯志华和胡海岩基于 Kane 方程, 建立起了含有三次几何及惯性非线性项的大范围直线运动梁动力学方程, 对梁一、二阶固有频率比接近 1:3 时所出现的动力行为进行了分析, 着重研究了该类模型在第一阶模态主参激共振与一、二阶模态间内共振联合作用下一些复杂的非线性动力行为, 但对参激振动稳定性问题未作深入的研究^[4]。对具 3:1 内共振梁的参激共振引起的非线性动力行为问题, Chin 及 Nayfeh^[4,5] 和 Kar 等^[6] 从不同的物理对象出发, 进行了较系统深入的研究。

本文利用多尺度法并结合笛卡尔坐标变换, 对基于 Kane 方程所建立起的包含有耦合三次几何及惯性非线性项的大范围直线运动梁动力学控制方程进行一次近似展开, 着重对含内共振现象的大范围运动两端饺支梁参激振动平凡解稳定性进行了详尽的分析与研究。

1 运动方程的建立

以两端饺支梁为图示参考模型。假设匀质梁 B 变形前所取与其轴线垂直截面变形后仍与变形后轴线垂直, 梁未变形前相对参考坐标系 R_1 单位矢量 a_1, a_2 分别平行、垂直其轴线。在

2001-04-27 收到第一稿, 2001-09-04 收到修改稿。

1) 国防基础科研计划项目(10172005)资助。

未变形梁轴线离点 O 距离 x 处取点 C_V ，变形后该点移至 C ，相对弹性变形向量为 \mathbf{u} ，如图 1 所示。取梁上与轴线垂直且包含 C 点的微段，则 C 点在 Newton 系中相对原点的矢径为

$$\mathbf{r}_N^C = \mathbf{r}_0 + \mathbf{r} + \mathbf{u} \quad (1)$$

式中 $\mathbf{r} = x\mathbf{a}_1$ ， $\mathbf{u} = u_1\mathbf{a}_1 + u_2\mathbf{a}_2$ 。

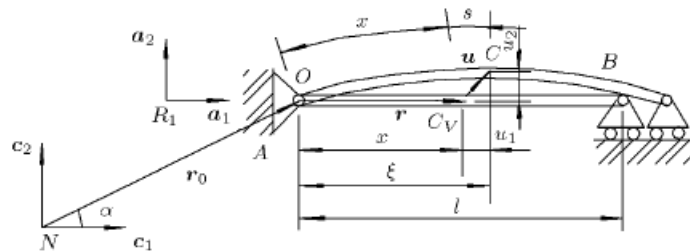


图 1 非惯性系中两端铰支梁

Fig.1 Configuration of a simply supported beam under a large linear motion of basement

当基础 A 为直线运动时，对式 (1) 求导得 C 点速度及相应的加速度分别为

$$\mathbf{v}_N^C = (v_0 \cos \alpha + \dot{u}_1)\mathbf{a}_1 + (v_0 \sin \alpha + \dot{u}_2)\mathbf{a}_2 \quad (2)$$

$$\mathbf{a}_N^C = (\ddot{v}_0 \cos \alpha + \ddot{u}_1)\mathbf{a}_1 + (\ddot{v}_0 \sin \alpha + \ddot{u}_2)\mathbf{a}_2 \quad (3)$$

式中 v_0 为基础 A 直线运动速度， α 为直线运动方向与未变形梁轴线夹角。

只考虑拉伸与弯曲变形，有

$$x + s = \int_0^x \sqrt{(1 + u_{1,\beta})^2 + (u_{2,\beta})^2} d\beta \quad (4)$$

假设梁为中等变形，故在后续的 Taylor 级数展开过程中保留至 $O(u_{1,x})$, $O(s_x)$ 及 $O(u_{2,x}^2)$ 项。对式 (4) 进行 Taylor 级数展开，近似有

$$u_1 = s - \frac{1}{2} \int_0^x (u_{2,\beta})^2 d\beta \quad (5)$$

采用 Rayleigh-Ritz 法，设

$$s(x, t) = \sum_{i=1}^{n_1} \Phi_{1i}(x) q_i(t), \quad u_2(x, t) = \sum_{i=1}^{n_2} \Phi_{2i}(x) Q_i(t) \quad (6)$$

式中 Φ_{1i}, Φ_{2i} 为未受约束时梁纵、横振动的固有振型函数， q_i, Q_i 为各自对应的广义坐标， n_1, n_2 为各自模态截断数。

经简化，梁的轴向力 P 及弯矩 M 分别为

$$P = EA_0 s_x \quad (7)$$

$$M = EI u_{2,xx} \left(1 - 2s_x + \frac{1}{2} u_{2,x}^2 \right) - EI s_{xx} u_{2,x} \quad (8)$$

式中 E, I 及 A_0 分别为梁的弹性模量、截面惯性矩及截面积。梁的势能 U 为

$$U = \int_0^l \frac{P^2}{2EA_0} dx + \int_0^l \frac{M^2}{2EI} dx \quad (9)$$

根据 Kane 方程，有

$$\int_0^l \rho \left(\mathbf{a}_N^C \cdot \frac{\partial \mathbf{v}_N^C}{\partial y_k} \right) dx + \frac{\partial U}{\partial y_k} = 0 \quad (10)$$

式中 y_k 为 q_k 或 Q_k 。

最终有

$$M_{1k}\ddot{q}_k + K_{1k}q_k - \sum_{i=1}^{n_2} \sum_{j=1}^{n_2} (2D_{1ij}^k + E_{1ij}^k)Q_iQ_j - \sum_{i=1}^{n_2} \sum_{j=1}^{n_2} C_{1ij}^k(\dot{Q}_i\dot{Q}_j + Q_i\ddot{Q}_j) = \\ -a_{1k}\dot{v}_0 \cos \alpha; \quad k = 1, 2, \dots, n_1 \quad (11)$$

$$M_{2k}\ddot{Q}_k + K_{2k}Q_k - \sum_{i=1}^{n_2} (a_{2i}^k \dot{v}_0 \cos \alpha)Q_i - \sum_{i=1}^{n_1} \sum_{j=1}^{n_2} C_{2ij}^k \ddot{q}_i Q_j - \sum_{i=1}^{n_1} \sum_{j=1}^{n_2} (4E_{2ij}^{k1} + E_{2ij}^{k2} + E_{2ij}^{k3})q_i Q_j + \\ \sum_{h=1}^{n_2} \sum_{i=1}^{n_2} \sum_{j=1}^{n_2} D_{2hij}^k(Q_h Q_i \ddot{Q}_j + Q_h \dot{Q}_i \dot{Q}_j) + \sum_{h=1}^{n_2} \sum_{i=1}^{n_2} \sum_{j=1}^{n_2} (F_{2ijh}^k + G_{2ijh}^k)Q_h Q_i Q_j = \\ -b_{2k}\dot{v}_0 \sin \alpha; \quad k = 1, 2, \dots, n_2 \quad (12)$$

式中

$$M_{1k} = \int_0^l \rho \Phi_{1k} \Phi_{1k} dx, \quad K_{1k} = \int_0^l EA_0 \Phi_{1k,x} \Phi_{1k,x} dx, \quad D_{1ij}^k = \int_0^l EI \Phi_{2i,xx} \Phi_{2j,xx} \Phi_{1k,x} dx \\ C_{1ij}^k = \int_0^l \phi_{ij} \Phi_{1k} dx, \quad E_{1ij}^k = \int_0^l EI \Phi_{2i,xx} \Phi_{2j,x} \Phi_{1k,xx} dx, \quad a_{1k} = \int_0^l \rho \Phi_{1k} dx \\ M_{2k} = \int_0^l \rho \Phi_{2k} \Phi_{2k} dx, \quad K_{2k} = \int_0^l EI \Phi_{2k,xx} \Phi_{2k,xx} dx, \quad a_{2i}^k = \int_0^l \rho \phi_{ik} dx \\ C_{2ij}^k = \int_0^l \rho \Phi_{1i} \phi_{jk} dx, \quad D_{2hij}^k = \int_0^l \rho \phi_{ij} \phi_{hk} dx, \quad E_{2ij}^{k1} = \int_0^l EI \Phi_{2j,xx} \Phi_{2k,xx} \Phi_{1i,x} dx \\ E_{2ij}^{k2} = \int_0^l EI \Phi_{1j,xx} \Phi_{2i,x} \Phi_{2k,xx} dx, \quad E_{2ij}^{k3} = \int_0^l EI \Phi_{1j,xx} \Phi_{2i,xx} \Phi_{2k,x} dx \\ F_{2ijh}^k = \int_0^l EI \Phi_{2i,xx} \Phi_{2k,xx} \Phi_{2j,x} \Phi_{2h,x} dx, \quad b_{2k} = \int_0^l \rho \Phi_{2k} dx \\ G_{2ijh}^k = \int_0^l EI \Phi_{2i,xx} \Phi_{2j,xx} \Phi_{2h,x} \Phi_{2k,x} dx, \quad \phi_{ij} = \int_0^x \Phi_{2i,\beta}(\beta) \Phi_{2j,\beta}(\beta) d\beta$$

2 一阶近似展开

假设 $\alpha = 0$ 且梁为细长梁，即不计及梁的纵向振动。为此，引入无量纲变量

$$\eta = \frac{x}{l}, \quad \tau = \frac{t\pi^2}{T}, \quad \vartheta_k = \frac{Q_k}{\lambda l} \quad (13)$$

式中 $T = \sqrt{\frac{\rho l^4}{EI}}$, $\bar{\lambda}$ 为尺度系数.

设 $v_0 = a_0 + \bar{a} \cos \Omega t$, 其中 a_0, \bar{a} 及 Ω 分别为基础 A 直线运动的平均加速度, 简谐振动加速度幅值及其角频率. 结合式(13)一起代入式(12)后, 对所得方程组引入线性变换 $\vartheta = \Phi y$, 其中 $\vartheta = \{\vartheta_1 \vartheta_2 \cdots \vartheta_{n_2}\}^T$, $y = \{y_1 y_2 \cdots y_{n_2}\}^T$, $\Phi = \{\varphi_1 \varphi_2 \cdots \varphi_{n_2}\}$ 为所得方程组派生系统对广义质量归一化振型矩阵. 最后, 解耦所得方程组并引入线性阻尼, 有

$$\begin{aligned} \ddot{y}_k + 2\epsilon\hat{\zeta}_k\dot{y}_k + \omega_k^2 y_k - \epsilon \sum_{i=1}^{n_2} \hat{b}_{2i}^k y_i \cos \omega \tau + \epsilon \sum_{i=1}^{n_2} \sum_{j=1}^{n_2} \sum_{h=1}^{n_2} \hat{\alpha}_{ijh}^k y_i y_j y_h + \\ \epsilon \sum_{i=1}^{n_2} \sum_{j=1}^{n_2} \sum_{h=1}^{n_2} \hat{\beta}_{ijh}^k (\dot{y}_j \dot{y}_h + y_j \ddot{y}_h) = 0; \quad k = 1, 2, \dots, n_2 \end{aligned} \quad (14)$$

式中

$$\begin{aligned} \hat{b}_{2i}^k &= \sum_{p=1}^{n_2} \sum_{h=1}^{n_2} \varphi_{pk} b_{2h}^p \varphi_{hi}, \quad \hat{\alpha}_{ijh}^k = \sum_{p=1}^{n_2} \sum_{l=1}^{n_2} \sum_{m=1}^{n_2} \sum_{n=1}^{n_2} \varphi_{pk} \alpha_{lmn}^p \varphi_{li} \varphi_{mj} \varphi_{nh} \\ \hat{\beta}_{ijh}^k &= \sum_{p=1}^{n_2} \sum_{l=1}^{n_2} \sum_{m=1}^{n_2} \sum_{n=1}^{n_2} \varphi_{pk} \beta_{lmn}^p \varphi_{li} \varphi_{mj} \varphi_{nh}, \quad \omega = \frac{\Omega T}{\pi^2}, \quad b_{2i}^k = \frac{\bar{a} T^2 \tilde{a}_{2i}^k}{\epsilon l \pi^4 \tilde{M}_{2k}} \\ \alpha_{ijh}^k &= \frac{\tilde{\alpha}_{ijh}^k}{\epsilon \tilde{M}_{2k}}, \quad \beta_{ijh}^k = \frac{\tilde{\beta}_{ijh}^k}{\epsilon \tilde{M}_{2k}}, \quad \tilde{M}_{2k} = \int_0^1 \Phi_{2k}^2 d\eta \\ \tilde{a}_{2i}^k &= \int_0^1 \phi_{ik} d\eta \quad \tilde{\beta}_{ijh}^k = \bar{\lambda}^2 \int_0^1 \phi_{ij} \phi_{hk} d\eta, \quad \phi_{ij} = \int_0^\eta \Phi_{2i,\beta} \Phi_{2j,\beta} d\beta \\ \tilde{\alpha}_{ijh}^k &= \frac{\bar{\lambda}^2}{\pi^4} \int_0^1 \Phi_{2i,\eta\eta} \Phi_{2j,\eta} (\Phi_{2h,\eta\eta} \Phi_{2k,\eta} + \Phi_{2h,\eta} \Phi_{2k,\eta\eta}) d\eta, \quad 0 < \epsilon \ll 1 \end{aligned}$$

采用多尺度法将 $y_k(\tau, \epsilon) = y_{k0}(T_0, T_1) + \epsilon y_{k1}(T_0, T_1)$ ($T_0 = \tau$, $T_1 = \epsilon \tau$, $k = 1, 2, \dots, n_2$) 代入式(14), 对其进行一次近似展开并令 ϵ^0 及 ϵ^1 前系数为零, 相应地求得

$$y_{k0} = A_k(T_1) \exp(i\omega_k T_0) + cc; \quad k = 1, 2, \dots, n_2 \quad (15)$$

式中 cc 表示前项共轭(下同). 而 y_{k1} 则可由下列方程组决定

$$\begin{aligned} D_0^2 y_{k1} + \omega_k^2 y_{k1} &= -2i\omega_k (\hat{\zeta}_k A_k + A'_k) \exp(i\omega_k T_0) + \\ \frac{1}{2} \sum_{m=1}^{n_2} \hat{b}_{2m}^k &\{ A_m \exp[i(\omega + \omega_m)\tau] + \bar{A}_m \exp[i(\omega - \omega_m)T_0] \} + \\ \sum_{m=1}^{n_2} \sum_{j=1}^{n_2} \sum_{h=1}^{n_2} &\{ (-\hat{\alpha}_{mjh}^k + \omega_j \omega_h \hat{\beta}_{mjh}^k + \omega_h^2 \hat{\beta}_{mjh}^k) A_m A_j A_h \exp[i(\omega_m + \omega_j + \omega_h)T_0] + \\ (-\hat{\alpha}_{mjh}^k - \omega_j \omega_h \hat{\beta}_{mjh}^k + \omega_h^2 \hat{\beta}_{mjh}^k) A_m \bar{A}_j A_h \exp[i(\omega_m - \omega_j + \omega_h)T_0] + \\ (-\hat{\alpha}_{mjh}^k + \omega_j \omega_h \hat{\beta}_{mjh}^k + \omega_h^2 \hat{\beta}_{mjh}^k) \bar{A}_m A_j A_h \exp[i(-\omega_m + \omega_j + \omega_h)T_0] + \\ (-\hat{\alpha}_{mjh}^k - \omega_j \omega_h \hat{\beta}_{mjh}^k + \omega_h^2 \hat{\beta}_{mjh}^k) \bar{A}_m \bar{A}_j A_h \exp[i(-\omega_m - \omega_j + \omega_h)T_0] \} + cc \\ k &= 1, 2, \dots, n_2 \end{aligned} \quad (16)$$

为进一步描述参激共振及一、二阶模态间3:1内共振情况，引入频率调谐因子 σ_1 及 σ_2 ，使

$$\omega = \omega_p + \omega_q + \varepsilon\sigma_1; \quad p, q = 1, 2, \dots, n_2 \quad (17)$$

$$\omega_2 = 3\omega_1 + \varepsilon\sigma_2 \quad (18)$$

将式(17),(18)代入式(16)并假定梁的前两模态与其它任意模态间不存在内共振现象，根据激励条件，可求得一次近似解表达式。

当 $p, q = 1, 2$ 时，产生第一阶模态主参激共振或一、二阶模态组合参激共振或第二阶模态主参激共振现象，由于阻尼的存在，最终只有梁的前两阶模态对系统的长期动力行为起作用。引进笛卡尔坐标变换

$$A_k(T_1) = \frac{1}{2}[U_k(T_1) - iV_k(T_1)]e^{-i\lambda_k}; \quad k = 1, 2 \quad (19)$$

最终，相应的第一阶模态主参激共振时系统的调制方程组为

$$\left. \begin{aligned} \omega_1(U'_1 + \hat{\varsigma}_1 U_1) + \frac{1}{2}\left(\omega_1\sigma_1 - \frac{1}{2}\hat{b}_{21}^1\right)V_1 + \frac{1}{4}\hat{b}_{22}^1 V_2 - \frac{1}{8}\sum_{i=1}^2 c_{1i}V_1(U_i^2 + V_i^2) + \\ \frac{1}{8}d_{12}[V_2(V_1^2 - U_1^2) + 2U_1V_1U_2] = 0 \\ \omega_1(V'_1 + \hat{\varsigma}_1 V_1) - \frac{1}{2}\left(\omega_1\sigma_1 + \frac{1}{2}\hat{b}_{21}^1\right)U_1 - \frac{1}{4}\hat{b}_{22}^1 U_2 + \frac{1}{8}\sum_{i=1}^2 c_{1i}U_1(U_i^2 + V_i^2) + \\ \frac{1}{8}d_{12}[U_2(U_1^2 - V_1^2) + 2U_1V_1V_2] = 0 \\ \omega_2(U'_2 + \hat{\varsigma}_2 U_2) + \frac{1}{4}\hat{b}_{21}^2 V_1 + \frac{1}{2}\omega_2(3\sigma_1 - 2\sigma_2)V_2 - \frac{1}{8}\sum_{i=1}^2 c_{2i}V_2(U_i^2 + V_i^2) - \\ \frac{1}{8}d_{21}V_1(3U_1^2 - V_1^2) = 0 \\ \omega_2(V'_2 + \hat{\varsigma}_2 V_2) - \frac{1}{4}\hat{b}_{21}^2 U_1 - \frac{1}{2}\omega_2(3\sigma_1 - 2\sigma_2)U_2 + \frac{1}{8}\sum_{i=1}^2 c_{2i}U_2(U_i^2 + V_i^2) + \\ \frac{1}{8}d_{21}U_1(U_1^2 - 3V_1^2) = 0 \end{aligned} \right\} \quad (20)$$

式中

$$d_{12} = \hat{\alpha}_{121}^1 + \hat{\alpha}_{211}^1 + \hat{\alpha}_{112}^1 - 2\omega_1^2\hat{\beta}_{211}^1 + \omega_1\omega_2(\hat{\beta}_{121}^1 + \hat{\beta}_{112}^1) - (\omega_1^2\hat{\beta}_{121}^1 + \omega_2^2\hat{\beta}_{112}^1)$$

$$d_{21} = \hat{\alpha}_{111}^2 - 2\omega_1^2\hat{\beta}_{111}^2$$

$$c_{kj} = \begin{cases} 3\hat{\alpha}_{kkk}^k - 2\omega_k^2\hat{\beta}_{kkk}^k, & j = k \\ 2(\hat{\alpha}_{kjj}^k + \hat{\alpha}_{jjk}^k + \hat{\alpha}_{jkj}^k) - 2\omega_j^2\hat{\beta}_{jkj}^k - 2\omega_k^2\hat{\beta}_{jjk}^k, & j \neq k \end{cases}$$

类似地, 一、二阶模态间组合参激共振时系统的调制方程组为

$$\left. \begin{aligned} & \omega_1(U'_1 + \hat{\varsigma}_1 U_1) + \frac{1}{4}\omega_1(\sigma_1 + \sigma_2)V_1 - \frac{1}{4}\hat{b}_{22}^1 V_2 - \frac{1}{8}\sum_{i=1}^2 c_{1i}V_1(U_i^2 + V_i^2) + \\ & \quad \frac{1}{8}d_{12}[V_2(V_1^2 - U_1^2) + 2U_1V_1U_2] = 0 \\ & \omega_1(V'_1 + \hat{\varsigma}_1 V_1) - \frac{1}{4}\omega_1(\sigma_1 + \sigma_2)U_1 - \frac{1}{4}\hat{b}_{22}^1 U_2 + \frac{1}{8}\sum_{i=1}^2 c_{1i}U_1(U_i^2 + V_i^2) + \\ & \quad \frac{1}{8}d_{12}[U_2(U_1^2 - V_1^2) + 2U_1V_1V_2] = 0 \\ & \omega_2(U'_2 + \hat{\varsigma}_2 U_2) - \frac{1}{4}\hat{b}_{21}^2 V_1 + \frac{1}{4}\omega_2(3\sigma_1 - \sigma_2)V_2 - \frac{1}{8}\sum_{i=1}^2 c_{2i}V_2(U_i^2 + V_i^2) - \\ & \quad \frac{1}{8}d_{21}V_1(3U_1^2 - V_1^2) = 0 \\ & \omega_2(V'_2 + \hat{\varsigma}_2 V_2) - \frac{1}{4}\hat{b}_{21}^2 U_1 - \frac{1}{4}\omega_2(3\sigma_1 - \sigma_2)U_2 + \frac{1}{8}\sum_{i=1}^2 c_{2i}U_2(U_i^2 + V_i^2) + \\ & \quad \frac{1}{8}d_{21}U_1(U_1^2 - 3V_1^2) = 0 \end{aligned} \right\} \quad (21)$$

同理, 第二阶模态主参激共振时系统的调制方程组

$$\left. \begin{aligned} & \omega_1(U'_1 + \hat{\varsigma}_1 U_1) + \frac{1}{3}\omega_1\left(\frac{1}{2}\sigma_1 + \sigma_2\right)V_1 - \frac{1}{8}\sum_{i=1}^2 c_{1i}V_1(U_i^2 + V_i^2) + \\ & \quad \frac{1}{8}d_{12}[V_2(V_1^2 - U_1^2) + 2U_1V_1U_2] = 0 \\ & \omega_1(V'_1 + \hat{\varsigma}_1 V_1) - \frac{1}{3}\omega_1\left(\frac{1}{2}\sigma_1 + \sigma_2\right)U_1 + \frac{1}{8}\sum_{i=1}^2 c_{1i}U_1(U_i^2 + V_i^2) + \\ & \quad \frac{1}{8}d_{12}[U_2(U_1^2 - V_1^2) + 2U_1V_1V_2] = 0 \\ & \omega_2(U'_2 + \hat{\varsigma}_2 U_2) - \frac{1}{4}\hat{b}_{22}^2 V_2 + \frac{1}{2}\omega_2\sigma_1V_2 - \frac{1}{8}\sum_{i=1}^2 c_{2i}V_2(U_i^2 + V_i^2) - \\ & \quad \frac{1}{8}d_{21}V_1(3U_1^2 - V_1^2) = 0 \\ & \omega_2(V'_2 + \hat{\varsigma}_2 V_2) - \frac{1}{4}\hat{b}_{22}^2 U_2 - \frac{1}{2}\omega_2\sigma_1U_2 + \frac{1}{8}\sum_{i=1}^2 c_{2i}U_2(U_i^2 + V_i^2) + \\ & \quad \frac{1}{8}d_{21}U_1(U_1^2 - 3V_1^2) = 0 \end{aligned} \right\} \quad (22)$$

当 $p = m > 2, q = n > 2$ 或 $p = n > 2, q = m > 2$ 时, 产生第 m, n 阶模态间组合参激或主参激共振现象, 其形式与文献 [2] 所述相同.

3 平凡解及其稳定性分析

取无量纲平均加速度 $a = -a_0 T^2 / \pi^4 l$, 无量纲简谐振动加速度幅值 $a_m = -\bar{a} T^2 / \pi^4 l$, 尺度系

数 $\bar{\lambda} = 0.01$, 小参数 $\varepsilon = 0.01$. 则梁的前两阶无量纲固有频率 ω_1, ω_2 及三倍的第一阶固有频率 $3\omega_1$ 随 a 变化曲线如图 2 所示. 表 1 列出了参激激励系数随 a_m 及 a 变化情况, 由于参激激励系数与 a_m 的关系在 a 确定时呈线性关系, 故表 1 只列出了 $a_m = 0.1a$ 时参激激励系数的变化情况.

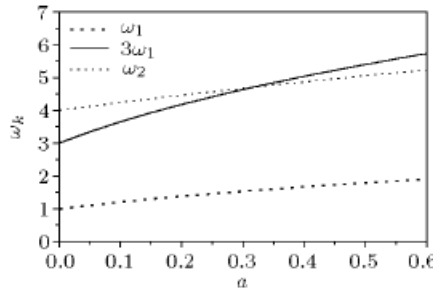
图 2 梁前两阶固有频率 ω_1, ω_2 及 $3\omega_1$ 随加速度 a 变化曲线

Fig.2 Variation of three times the first natural frequency ω_1 and the second natural frequency ω_2 with the axial acceleration a

表 1 \bar{a} 及 a 的变化对参激激励系数的影响

Table 1 Coefficients of parametric excitation

a	a_m	$\varepsilon\sigma_2$	\hat{b}_{21}^1	\hat{b}_{22}^1	\hat{b}_{21}^2	\hat{b}_{22}^2
0.2715	0.02715	0.1	12.0378	9.4390	9.4390	54.9495
0.3160	0.03160	-1.96×10^{-7}	13.8461	10.6007	10.6007	64.1308
0.3643	0.03643	-0.1	15.7718	11.7598	11.7598	74.1205

对形如二阶模态以上的组合或主参激共振的平凡解稳定性问题, 文献 [2] 已给出了解析的临界曲线表达式. 对于式 (20)~(22), 其平凡解的 Jacobi 矩阵特征多项式具有相同形式

$$\lambda^4 + C_1\lambda^3 + C_2\lambda^2 + C_3\lambda + C_4 = 0 \quad (23)$$

其中 $C_1 = 2(\hat{\zeta}_1 + \hat{\zeta}_2) > 0$; C_2, C_3 及 C_4 为由多参数决定且各不相同的系数.

将纯虚根 $\lambda = i\bar{\omega}$ 代入式 (23), 分离实、虚部, 得实根 $\bar{\omega}$ 所需满足条件即为平凡解临界稳定性的条件

$$\left. \begin{array}{l} f_1 : C_4 = 0 \\ f_2 : C_3^2 - C_1C_2C_3 + C_1^2C_4 = 0 \\ f_3 : C_3 = 0 \end{array} \right\} \quad (24)$$

3.1 第一阶模态主参激共振时系统稳定区域

图 3 显示了第一阶模态主参激共振时系统平凡解稳定性区域随参激激励幅值、激励频率、阻尼、内共振频率调谐因子等参数的变化情况, 曲线的 V 型内区为不稳定区域 (下同). 随着 σ_2 从负变正, 由内共振引起的窄小不稳定区域 II、III 从主参激共振不稳定区域 I 的左侧 (图 3(a)) 移至右侧 (图 3(c)). 区域 I、III 由条件 f_1 决定, 平衡点为鞍点, 而区域 II 由条件 f_2 决定, 平衡点为不稳定焦点. 在内共振完全调谐时, 稳定性区域基本由条件 f_1 决定. 条件 f_3 在所分析数值范围内对系统的稳定性未起决定性影响.

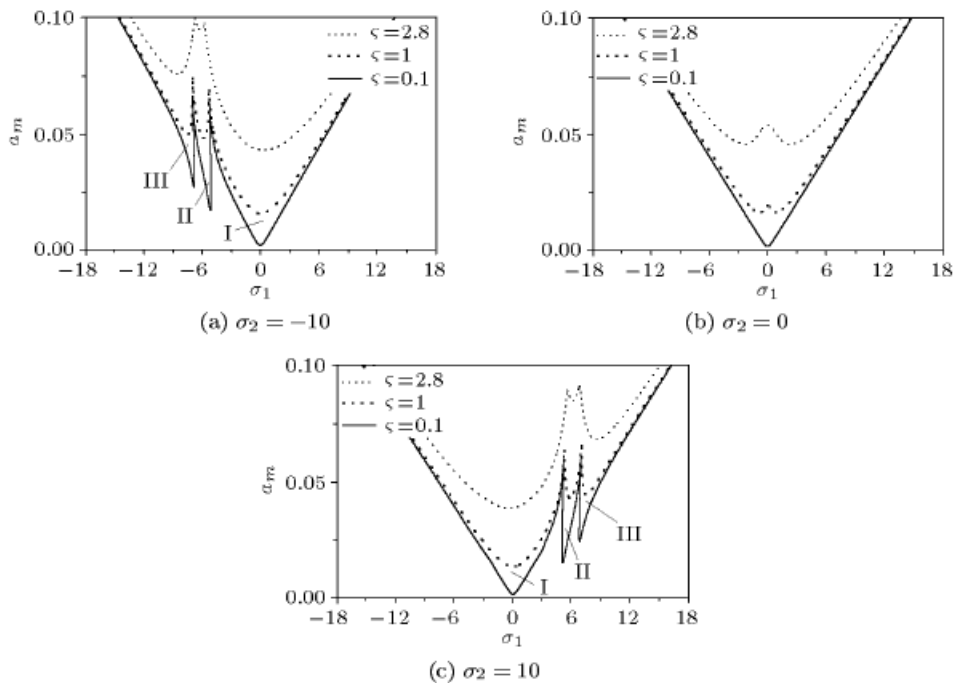
图 3 $\omega = 2\omega_1 + \varepsilon\sigma_1$, $\omega_2 = 3\omega_1 + \varepsilon\sigma_2$ 时稳定区域随参数 ζ ($\zeta = \zeta_1 = \zeta_2$) 及 σ_2 变化情况

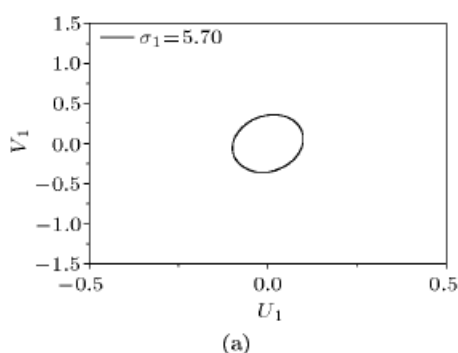
Fig.3 Stability diagram of principal parametric resonance at the first natural frequency

为了确定平衡点随参数 σ_1 变化从稳定区间进入不稳定区间 II 时的分岔类型, 将调谐方程(20)在奇异点处向中心流形投影, 获得降维的二维系统, 再采用 PB 规范型及极坐标变换^[7], 得标准形式

$$\left. \begin{array}{l} r' = \varepsilon_1(\sigma_1 - \sigma_{1c})r + \alpha_1 r^3 \\ \theta' = \omega_0 + \varepsilon_2(\sigma_1 - \sigma_{1c}) + \alpha_2 r^2 \end{array} \right\} \quad (25)$$

其中 r 为极限环半径, σ_{1c} 为相应奇异值, ε_1 为特征值实部穿越虚轴时对 σ_1 的导数, ω_0 为特征值在 σ_{1c} 时虚部值, α_1, α_2 及 ε_2 为相应参数.

根据 Poincaré-Andronov-Hopf 定理, 当 $\varepsilon_1(\sigma_1 - \sigma_{1c})\alpha_1 < 0$ 时系统产生极限环, 其稳定性与平衡点相反. 现以图 3(c) 为例, 即 $a = 0.2715$, 取 $a_m = 0.02715$, $\zeta = 0.1$, 此时 σ_{1c} 分别为 5.7380 及 5.0541. 经计算, ε_1 分别为 -4.1102 及 4.2017, α_1 为 -53.407 及 4.5684. 故 σ_1 减小并通过 5.7380 时产生 Hopf 分岔, 形成稳定极限环, 而减小穿过 5.0541 时所产生的极限环不稳定. 图 4 显示了 σ_1 在 5.7380 与 5.0541 间系统平凡响应所产生的极限环演变过程.

图 4 σ_1 在 5.7380 与 5.0541 间系统平凡响应所产生的极限环变化过程Fig.4 Two-dimensional projections of the phase portraits onto the U_1-V_1 plane for σ_1 between 5.7380 and 5.0541

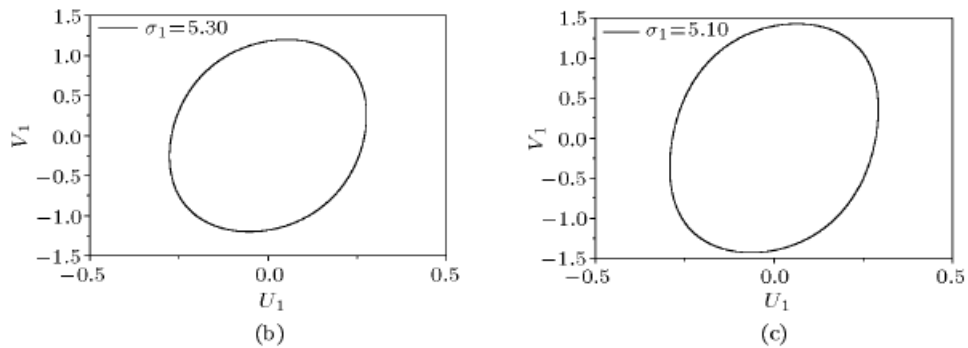
图4 σ_1 在 5.7380 与 5.0541 间系统平凡响应所产生的极限环变化过程(续)

Fig.4 Two-dimensional projections of the phase portraits onto the U_1 - V_1 plane for σ_1 between 5.7380 and 5.0541 (continued)

3.2 一、二阶模态间组合参激共振时系统稳定区域

由式(24)经分析得知,一、二阶模态间组合参激共振时平凡解稳定性区域边界由条件 f_2 决定,相应表达式见式(26),在不稳定区域内平衡点为不稳定焦点。从图5可看出,稳定区域对阻尼较敏感,但内共振频率调谐因子对其影响很小。

$$\sigma_1 = \pm \frac{1}{4} \sqrt{\frac{\omega_1 \omega_2 \hat{\zeta}_1 \hat{\zeta}_2 (\hat{b}_{21}^2 \hat{b}_{22}^1 - 16 \omega_1 \omega_2 \hat{\zeta}_1 \hat{\zeta}_2)(\hat{\zeta}_1 + \hat{\zeta}_2)}{\omega_1 \omega_2 \hat{\zeta}_1 \hat{\zeta}_2}} \quad (26)$$

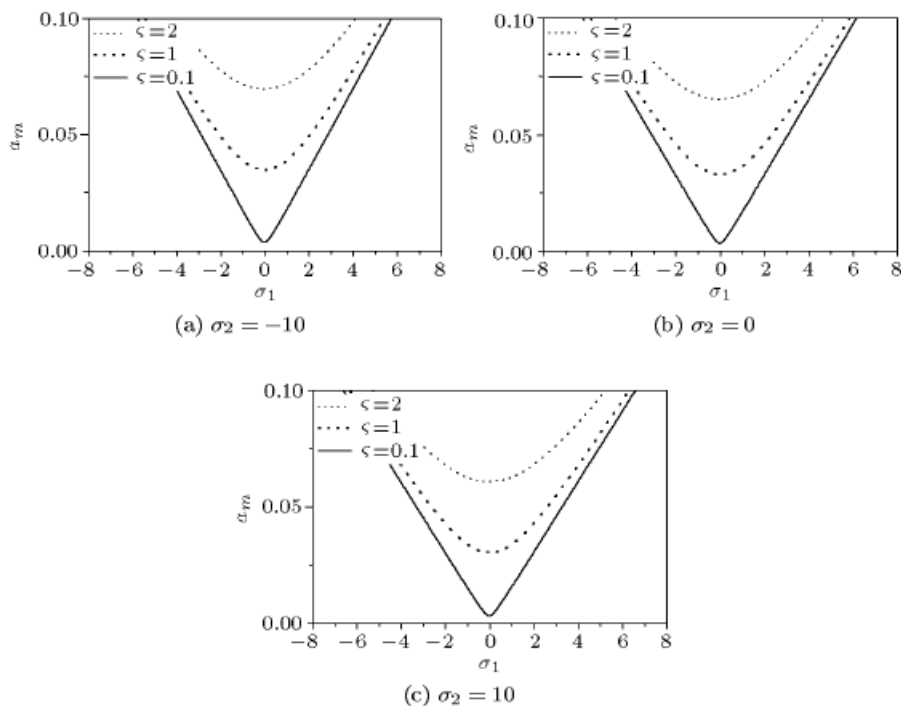
图5 $\omega = \omega_1 + \omega_2 + \varepsilon \sigma_1$, $\omega_2 = 3\omega_1 + \varepsilon \sigma_2$ 时稳定区域随参数 ζ ($\zeta = \hat{\zeta}_1 = \hat{\zeta}_2$) 及 σ_2 变化情况

Fig.5 Stability diagram of combination parametric resonance between the first two natural frequencies

3.3 第二阶模态主参激共振时系统稳定区域

第二阶模态主参激共振时平凡解稳定性区域边界由条件 f_1 决定, 相应表达式见式(27), 在不稳定区域内平衡点为鞍点. 此时系统的平凡响应呈单模态状态, 即无论第二阶模态的零解稳定与否, 第一阶模态的平凡响应始终是稳定的. 另外, 从式(22)可看出, 对于稳定的第一阶模态的平凡解, 第二阶模态存在两非平凡解, 此时, 一、二阶模态间并未因存在内共振而被相互激发起来, 对应的第二阶非平凡解见式(28). 图6实质为第二阶模态主参激共振平凡响应的稳定区域图, 从中可看出, 阻尼、内共振频率调谐因子对稳定区域影响较前两种情况要小得多.

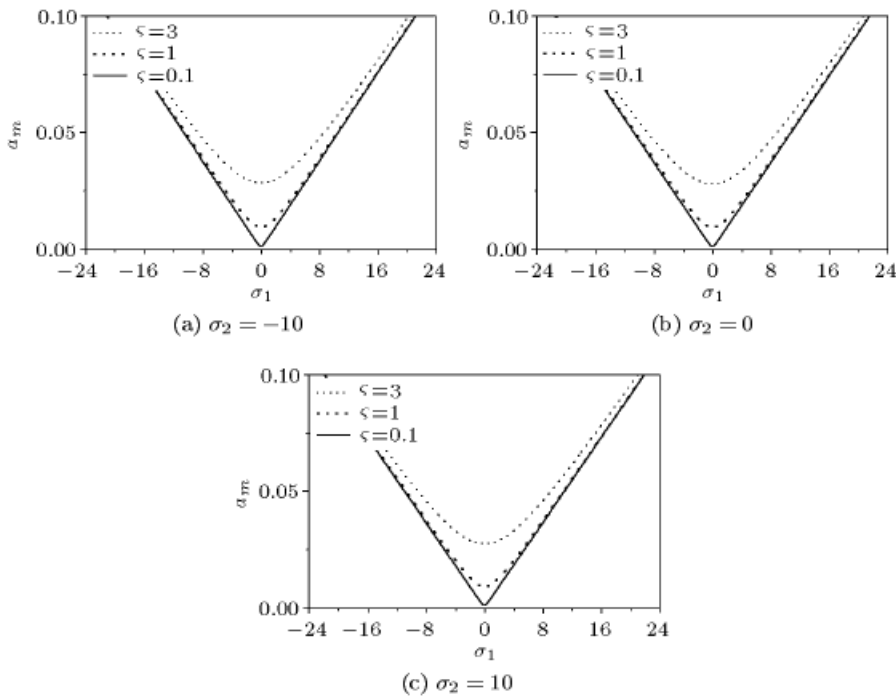


图 6 $\omega = 2\omega_2 + \varepsilon\sigma_1$, $\omega_2 = 3\omega_1 + \varepsilon\sigma_2$ 时稳定区域随参数 ζ ($\zeta = \hat{\zeta}_1 = \hat{\zeta}_2$) 及 σ_2 变化情况

Fig.6 Stability diagram of principal parametric resonance at the second natural frequency

$$\sigma_1 = \pm \frac{1}{2} \sqrt{\left(\hat{b}_{22}^2\right)^2 - 16\omega_2^2\zeta_2^2} \quad (27)$$

$$a_2^2 = \frac{4\omega_2}{c_{22}} \left(\sigma_1 \pm \sqrt{\left(\frac{\hat{b}_{22}^2}{2\omega_2}\right)^2 - (2\hat{\zeta}_2)^2} \right) \quad (28)$$

式中 $a_2^2 = U_2^2 + V_2^2$.

4 结束语

由于一、二阶模态间存在 3:1 内共振情况, 使得大范围直线运动梁的动力行为变得十分复杂, 其平凡解稳定性也不例外.

对于二阶以上模态的主参激共振或组合参激共振梁，平凡解稳定性未受前两阶模态间存在的内共振的影响。而当在第二阶模态附近产生参激激励时，系统最主要的特征是其呈现单模态现象，即对应第一阶模态的平凡响应，第二阶模态有一个平凡解，两个非平凡解。当参激激励频率接近一、二阶固有频率之和时，所导致平凡解的不稳定区域对阻尼较敏感，另外，在不稳定区域内的平凡稳态响应为不稳定焦点。当参激激励频率接近两倍的第一阶固有频率时，平凡稳态响应的稳定性较复杂，除了有不稳定的主共振区外，还增加了数个窄小的不稳定区域，导致其产生新的叉形分岔及 Hopf 分岔，而且这些不稳定区域与内共振调谐程度紧密相关。

参 考 文 献

- 1 Kane TR, Ryan RR, Banerjee AK. Dynamics of a cantilever beam attached to a moving base. *Journal of Guidance, Control, and Dynamics*, 1987, 10(2): 139~151
- 2 Nayfeh AH, Mook DT. Nonlinear Oscillations. New York: John Wiley & Sons, 1979. 304~321
- 3 Hyun SH, Yoo HH. Dynamic modeling and stability analysis of axially oscillating cantilever beams. *Journal of Sound and Vibration*, 1999, 228(3): 543~558
- 4 Chin CM, Nayfeh AH. Three-to-one internal resonances in hinged-clamped beams. *Nonlinear Dynamics*, 1997, 12(2): 129~154
- 5 Chin CM, Nayfeh AH. Three-to-one internal resonances in parametrically excited hinged-clamped beams. *Nonlinear Dynamics*, 1999, 20(2): 131~158
- 6 Kar RC, Dwivedy SK. Non-linear dynamics of a slender beam carrying a lumped mass with principal parametric and internal resonances. *International Journal of Non-Linear Mechanics*, 1999, 34(3): 515~529
- 7 胡海岩. 应用非线性动力学. 北京: 航空工业出版社, 2000. 152~159 (Hu Haiyan. Applied Nonlinear Dynamics. Beijing: Aviation Industry Press, 2000. 152~159 (in Chinese))

DYNAMIC STABILITY OF A SLENDER BEAM WITH INTERNAL RESONANCE UNDER A LARGE LINEAR MOTION¹⁾

Feng Zhihua Hu Haiyan

(Institute of Vibration Engineering Research, Nanjing University of Aeronautics and Astronautics,
Nanjing 210016, China)

Abstract Dynamic modeling of a flexible beam undergoing a large linear motion is presented in this paper at first. The equations of motion for the beam are derived by using Kane's equation and then simplified through the Rayleigh-Ritz method. Different from the linear modeling method where the generalized inertia forces and the generalized active forces are linearized in the modeling process, the present model takes the coupled cubic non-linearities of geometrical and inertial types into consideration. In the case of a simply supported slender beam under certain average acceleration of base, the second natural frequency of the beam may approximate to the tripled first one so that the condition of 3:1 internal resonance of the beam holds true. The method of multiple scales is used to solve directly the nonlinear differential equations and to derive the nonlinear

Received 27 April 2001, revised 4 September 2001.

1) The project supported by the Fundamental Research Fund of National Defence (10172005).

modulation equation for either the principal parametric resonance or the combination parametric resonance with 3:1 internal resonance between the first two modes of the beam. The dynamic stability of the trivial state of the system is investigated by using Cartesian transformation in detail. The equations of approximate transition curves in the plane of dimensionless frequency and excitation parameter that separate stable from unstable solution are derived. For the case of principal parametric resonance of the first mode, in addition to the principal instability region, there exist several new narrow instability regions because of the presence of internal resonance. These narrow regions move from the left of the principal instability region to the right of it when the frequency detuning parameter of internal resonance increases from the negative to the positive. In contrast with the case of principal parametric resonance of the first mode, single mode equilibrium solution is possible for the principal parametric resonance of the second mode. Furthermore, the stability of the trivial solution for the third mode or the higher ones has not been affected by the internal resonance between the first two modes. Finally, the modulation equations are reduced to a two-dimensional system and the type of a Hopf bifurcation is determined in the vicinity of the bifurcation via the center manifold theorem and a limit cycle is found.

Key words beam, dynamic stability, parametric excitation, internal resonance, method of multiple scales, large linear motion